OPTOELECTRONICS AND ADVANCED MATERIALS – RAPID COMMUNICATIONS Vol. 7, No. 11-12, November - December 2013, p. 965-975

Sintering, microstructure and dielectric properties of MgO doped alumina ceramics co-doped with Gd_3O_2, and Pr_6O_2

G. RAMESH[a,*], R. V. MANGALARAJA[b], S. ANANTHAKUMAR[c], P. MANOHAR[a]
[a]*Department of Ceramic Technology, AC Tech. Campus, Anna University, Chennai, India*
[b]*Department of Materials Engineering, University of Concepcion, Concepcion, Chile*
[c]*Materials and Minerals Division, National Institute for Interdisciplinary Science and Technology (NIIST), Trivandrum, India*

There is a need for low dielectric, low loss ceramic substrates for microwave electronics. Earlier works report rare earth dopants are very much useful to control the dielectric properties of sintered ceramics. This paper describes the effect of Gd_2O_3 and Pr_2O_6 rare earth co-dopants on the dielectric properties of MgO-doped alumina ceramics. Sintering, microstructures and the dielectric properties are investigated and reported. First of all, ultrafine alumina particles were obtained by ball milling which were converted to sintered alumina ceramics at temperatures 1400, 1450, 1500 and 1550^oC. Sintered α -Al_2O_3 ceramics showed nearly 70% theoretical sintered density at 1450 °C which was increased beyond 97% at 1550 °C. The SEM micro-structure images reveal the presence of elongated, spherical like Al_2O_3 grains in the sintered samples. The results on dielectric constant (ε_r), dielectric loss and a.c. resistivity indicate that sintered MgO doped alumina ceramics have low dielectric constant in the range ε_r <6 in presence of Gd_2O_3 and Pr_2O_6 co dopants which is one order less than the phase pure Al_2O_3 ceramics. The dielectric constant decreases with the increase in MgO. The resistivity of sintered alumina increases with increase in dopant concentration and decreases with increase in temperature. High vacancy concentration at the interfaces of GPMDA and Al_2O_3 phases is possibly responsible for the resistivity of G-P co doped Al_2O_3 ceramics. The fine grain microstructure of sintered alumina creates more interfaces which in turn responsible for the dielectric constant 4.9 to 8.7 for doped alumina at the frequency of 1 MHz.

(Received August 1, 2013; accepted November 7, 2013)

Keywords: Sintering, dielectric properties, Dielectric Loss, Dielectric constant, Alumina

1. Introduction

The developments in the microelectronic industry accelerate the search for new material with innovative properties which can fulfil the requirements of technological advances. The dielectric ceramics play a prominent role in telecommunication and satellite broadcasting industry for its potential advantages such as reliability, ease of integration, good dielectric properties and excellent performance. The basic requirements of materials for RF applications are low dielectric loss, optimum relative permitivity and nearly zero temperature coefficient of resonant frequency. In electronic industry, dielectric materials are being used as electronic packaging applications, substrates, dielectric resonators, waveguides, dielectric antennas and capacitors etc [1-4].

Alumina (Al_2O_3) is widely used in the electronics industry for passive components such as interconnection, resistances, and capacitors and is specifically employed in applications such as substrates for hybrid circuits, multi-layer interconnection circuits, microelectronic packaging, sensors etc. some of the dielectric materials for substrate applications such as chromium doped alumina Thorp et. al. [5], alumina filled epoxy Naoki et. al., [6] and micro and nano alumina filled silicone rubber Namitha et. al., [7] were investigated.

The investigation on the usage of Alumina for electronic applications has been started in the early stage by Thorp et. al., (1990). They studied the dielectric properties for pure and chromium doped single crystal alumina in the applied frequency range of 0.5 KHz to 10 MHz. Cheng-Liang Huang et. al., (2005) reported that nano α-Alumina (sintered at 1550°C) has a dielectric constant of ε_r=10. In 2008, Cheng-Liang Huang et al reported nano (Θ +α)-Al_2O_3 ceramics dielectric constant =10 sintered at 1400 °C for 8 hrs frequency of 14 GHz. Jin-min Chen et.al., [8] reported 20 wt% $CaSiO_3$ addition in alumina possessed dielectric properties of ε_r = 6.59 at 1340 °C. Later Jozef Chovanec et. al., [9] reported the addition of 0.05 and 0.5 wt.% of MgO and CaO in alumina decreased the value of loss tangent in the whole frequency range between 1 and 200 KHz. Namitha et. al., (2013) reported the micro alumina has a relative permittivity (ε_r) of 5.89 and dielectric loss of 9×10^{-3} for silicone rubber composite filled with micro alumina.

2. Experimental

To achieve porous ceramics with fine-grained and fully dense matrix, five sets of doped alumina, were prepared using solid state reaction technique. First, High purity commercial calcined alumina powder (Hindalco, India) was used as base material. For doping alumina, magnesium oxide (Merck, India), praseodymium oxide(CDH, India), Gadolinium oxide (CDH, India) and Boehmite were selected in different compositions as shown in Table 1.

Table 1. Selection of Batches and dopant compositions.

Sl. No	Batches	Composition
1	Batch I	Pure alumina
2	Batch II	0.5 mol % MgO+ 0.3 mol % Pr_2O_3+0.3 mol % Gd_6O_2 doped in Al_2O_3
3	Batch III	0.3 mol % MgO+ 0.5 mol % Pr_2O_3+0.3 mol % Gd_6O_2 doped in Al_2O_3
4	Batch IV	0.3 mol % MgO+ 0.3 mol % Pr_2O_3+0.5 mol % Gd_6O_2 doped in Al_2O_3
5	Batch V	Alumina + 15 wt % Boehmite

For better mixing and size reduction of the powder, the alumina and dopant powders were weighed in different molar ratio proportions and the mixture were wet-milled in iso-propanal for 10 h in a High energy ball mill with tungsten carbide balls. The particle size of before and after milling were measured with the help of Laser Diffraction Technique instrument (LA950,HORIBA Instruments, inc. U.S.A).The dried powders were mixed with an organic binder (polyvinyl alcohol) 2 wt%, and the mixtures were pressed into pellets of 13 mm diameter and 2 mm thickness by applying a pressure of 5 ton. Four sintering temperatures, 1400, 1450, 1500 and 1550 °C were selected for all batch compositions. The pellets of each composition were fired in an electrically heated muffle furnace (Nabertherm, Germany) with a heating schedule of 3 °C/min up to 600 °C, maintained constant 600 °C for 20 minutes and then 3 °C/min up to respective firing temperature with 2 h soaking. Forced cooling was done up to 800°C with exhaust fan attached to the furnace, and afterwards normal cooling up to room temperature. The physical properties such as bulk density and porosity of the sintered pellets were measured by the Archimedes principle. The formations of crystalline phases of the sintered ceramics were identified by XRD using CuKa radiation with a General Engineering X-ray diffractometer (model GE-110T). The crystalline phase size was determined from peak broadening using the following relation

$$d = \frac{0.9\,\lambda}{B\cos\theta} \quad (1)$$

d = phase size, A°
λ = wavelength of X-ray = 1.542A°
B = full width at half maximum, radians
θ = position of X-ray peak

Silicon was also employed as an external standard for correction due to instrumental broadening. The microstructure photographs were recorded in scanning electron microscope for topography studies of the sintered alumina ceramics.

The a.c. resistivity, the dielectric constants ε_r, as well as dielectric loss of the samples were carried out at room temperature (30 °C) at different frequencies ranging from 350 Hz to 3 MHz using the following relation.

Dielectric constant (ε_r') was evaluated by using the following relation:

$$\varepsilon_r' = C/Co \quad (2)$$

where C and C_o were the capacitance values with and without sample, respectively, C_o is given by= [(0.08854 A)/d] pF; where A (cm^2) is the area of the electrodes and d (cm) is the thickness of the sample

Dielectric loss (ε_r'') was evaluated by the following relation:

$$\varepsilon_r'' = \tan\delta \;\; \varepsilon_r' \quad (3)$$

where tanδ is the dissipation factor, ε_r' is the dielectric constant a.c. conductivity of ultrafine alumina sample was calculated by using the following relation:

$$\sigma_{a.c.} = \varepsilon_o\, \omega\, \varepsilon' \tan\delta$$
$$\rho\ a.c. = \frac{1}{\sigma\ a.c.} \quad (4)$$

where tanδ is the dissipation factor, ω is the angular frequency, which is equal to 2πf (where f is the frequency) and ε_o is the relative permittivity of free space.

The surfaces of each sintered pellet were carefully polished and then coated with silver paint. Before

conducting the experiment, the surfaces were checked for good contact. The computerised LCR bridge (Hioki 3532-50 Hi tester) was used to measure the electrical properties of the samples.

3. Results and discussion

3.1 Characterisation of alumina powder

Particle size distribution (Table 2) of alumina reveals that most part of the powder is in submicron level, and around 80 wt% of the material in the range 800 nm to 132 nm (in Table 1, cumulative % values at an interval of 10 have been listed as the total data set is quite voluminous). This fineness in size confirms the sinter-active nature of the powder at the firing temperatures 1400, 1450, 1500 and 1550°C [10]. Fig. 1 and Fig. 2 shows the particle size distribution of powder before and after high energy ball milling.

Table 2. Particle size distribution of calcined technical alumina powder (report by mass %).

Cumulative mass finer %	Low diameter (μm)	
	As received calcined powder	Milled powder 600 min.
10	0.2596	0.1321
20	0.3507	0.1748
30	0.5661	0.2171
40	1.7282	0.2667
50	15.1344	0.3329
60	64.4549	0.4355
70	89.5735	0.5877
80	120.4539	0.8064
90	187.8522	1.2060

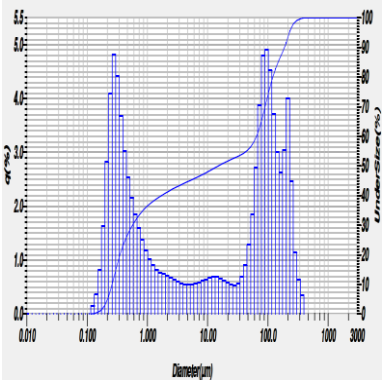

Fig. 1. Particle size distribution of powder Before high energy ball milling.

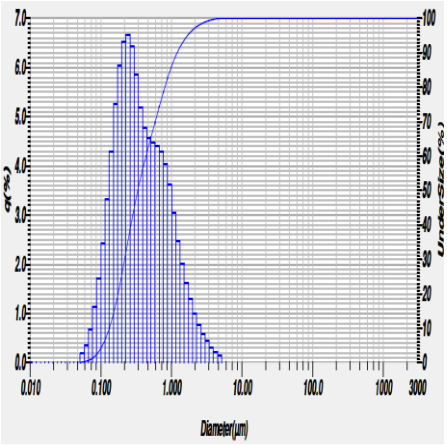

Fig. 2. Particle size distribution of powder after high energy ball milling.

3.2 Sintering and densification

The present work reveals that not only amount of additive but also its nature plays some role to achieve maximum density during sintering. Beyond powder granulometry, amount and nature of additive additions; other parameters like forming process, firing schedule (temperature, time and heating rate) and firing atmosphere are equally effective to attain bulk density of the sintered bodies [11]. Improved forming process such as isostatic pressing and rare earth element such as praseodymium oxide and Gadolinium oxide as sintering additives will help to stop secondary grain growth to a greater extent of alumina and it is possible to achieve ρth density. Difference in sintering behaviour of alumina with types of addition of additives may also introduce some change in material properties of the sintered pellets. During sintering process, the MgO, rare earth elements such as Pr_6O_2 and Gd_3O_2 react with alumina grains and form magnesium incorporated aluminium oxides, which is a liquid phase at elevated temperature. With the help of reaction- derived liquid of magnesium incorporated aluminium oxides, the alumina grains are dragged close with each other. The rare earth additives content in the green body, it is having pinning effect and inhibited the growth of alumina grains are dragged together, so that small size of grains were developed [12] as shown in the proposed model in Fig. 3.

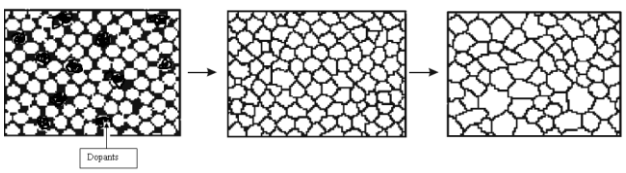

Fig. 3. Structural changes in a powder pellet during sintering due to pinning effect of rare earths additives.

Linear shrinkage was determined by measuring the maximum diameter of the circular samples after cold

pressing and before sintering (L_o) and the maximum diameter of the specimen after sintering (L).The linear shrinkage was calculated by the formula:

$$Linear\ shrinkage = \frac{(L - Lo)}{Lo} \ \%$$

In α-Al_2O_3, as the content of MgO, Pr_6O_2 and Gd_3O_2 in the green body increases from 0.3 mol % to 0.5 mol % in Al_2O_3 increases in volume shrinkage from 4 to 18% and decreases in porosity from 28 to 6%. The relative density also increases in different composition from 62 to 98 % as shown in Fig. 3, Fig. 4 and Fig. 5.

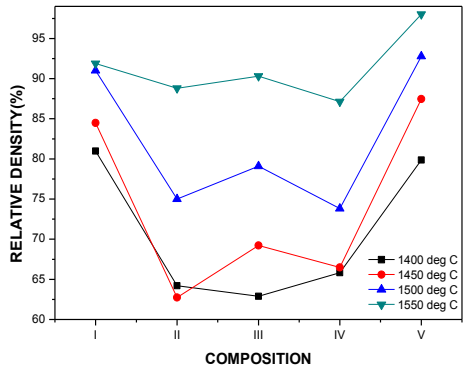

Fig. 3. Composition Vs relative density.

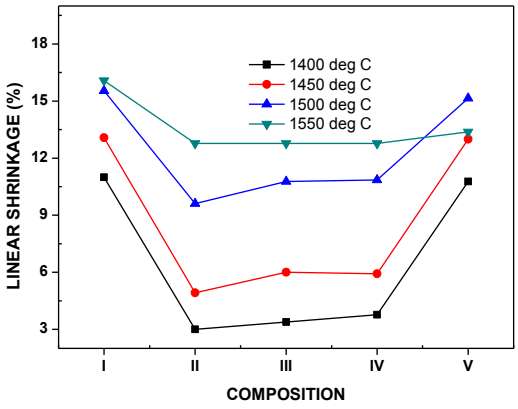

Fig. 4. Composition Vs % of linear shrinkage.

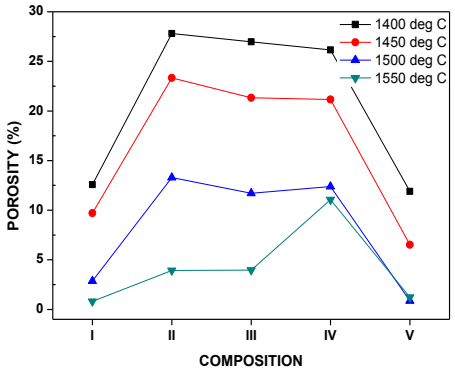

Fig. 5. Composition Vs % of porosity XRD analysis.

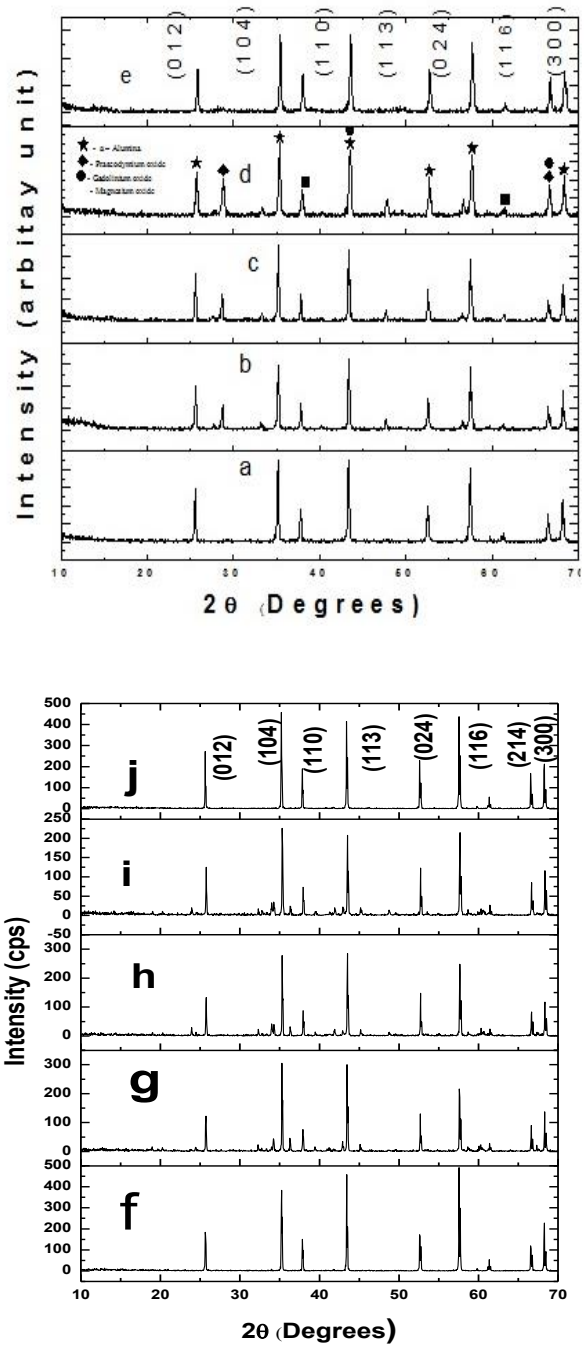

Fig. 6. XRD patterns of Al_2O_3 powder Batch-I,b) Batch II (c) Batch III (d) Batch IV (e) Batch V XRD patterns of 1450 °C conventional sintered Al_2O_3 pellet f) Batch-I, (g) Batch II (h) Batch III (i) Batch IV (j) BatchV.

The crystalline phases present in our samples were investigated by X-ray powder diffraction (XRPD) using Cu Ka radiation at a rate of 60/min on a General Engineering X-ray diffractometer, (model GE-110T). Silicon was also employed as an external standard for correction due to instrumental broadening.

The preparation of samples was accomplished by sintering the ultrafine α-Al_2O_3 ceramics added with various

amounts of additives MgO- Pr_2O_3-Gd_6O_2 at temperatures of 1450–1550 °C. Fig. 6 shows the XRD pattern of various amounts of additives MgO- Pr_2O_3-Gd_6O_2 added in alumina powder XRD pattern of sintered pellet at different temperatures. The crystal systems of α -Al_2O_3 (JCPDS #82–1468), MgO(JCPDS #21–1276), Pr_6O_2 (JCPDS #71-0341) and Gd_3O_2(JCPDS #86–2477) are hexagonal, cubic, hexogonal, and monoclinic, respectively. The broad peaks suggest the presence of small particle sizes. Particle sizes of prepared powders and sintered pellet calculated from X-ray peak broadening of the (104) diffraction peak using the Scherrer formula are about 49-75 nm for all compositions and sintered pellet ranges from 1.11 to 97.84 nm.

In fact, an MgO, Pr_2O_3 and Gd_6O_2 peak, as it appeared in Figs. 6(b) to (d), was identified without any second phase for all specimens tested in the experiment. Moreover, additives crystalline phases are disappear in 1450 °C sintered sample. However, the eradication of the additives emerged and only Al_2O_3 were detected at 1450°C in our experiments. It was attributed to smaller starting powders, resulting in a faster reaction between reacting constituents.

Table 2. Lattice constant and crystalline phase size of powders and sintered pellets.

Batch.	Composition	Crystalline phase size(nm) For (104) plane	
		Powder	Sintered pellet
I	Pure alumina	75.30	1.33
II	Composition I (0.5 mol % MgO+ 0.3 mol % Pr_2O_3+0.3 mol % Gd_6O_2 doped in Al_2O_3)	66.59	1.20
III	Composition II (0.3 mol % MgO+ 0.5 mol % Pr_2O_3+0.3 mol % Gd_6O_2 doped in Al_2O_3)	77.07	96.132
IV	Composition III (0.3 mol % MgO+ 0.3 mol % Pr_2O_3+0.5 mol % Gd_6O_2 doped in Al_2O_3)	49.45	1.11
V	Alumina + Boehmite	68.71	97.84

3.4 Microstructure analysis

The SEM micrographs of the α-Al_2O_3 ceramics at different sintering temperatures are illustrated in Fig. 7. The as-sintered surfaces were porous and the samples exhibited small grain size when sintered at 1400 °C. With the increase in sintering temperature, the number of pores decreased and the rate of grain growth apparently increased. These may directly affect the microwave dielectric properties of the ceramic samples.

The relative densities of the α-Al_2O_3 ceramics at different sintering temperatures are indicated in Fig. 3. For a pure α-Al_2O_3 sintered ceramics a low relative density of 81% was obtained at 1400 °C due to the porous specimen as shown in Fig. 7. However, the relative density increased and started to saturate at 1550 °C (relative density= 92%) with increasing sintering temperature. In the case of Batch I sintered material have a low relative density of 65% at 1400 °C and increase to 91% for the temperature of 1550 °C. For Batch II at 1400 °C the relative density was obtained 64 % and increased to 92 % for the temperature of 1550 °C. From Batch III sintered sample observed that at 1400 °C the relative density was 67% and increased to 89% for 1550 °C. For the Boehmite addition sintered pellet, the relative density improved from 87% at 1400 °C to 98% at 1550 °C.

The increase in relative density with increasing sintering temperature was attributed to the decrease in the number of pores as well as grain growths were observed in Fig. 7.

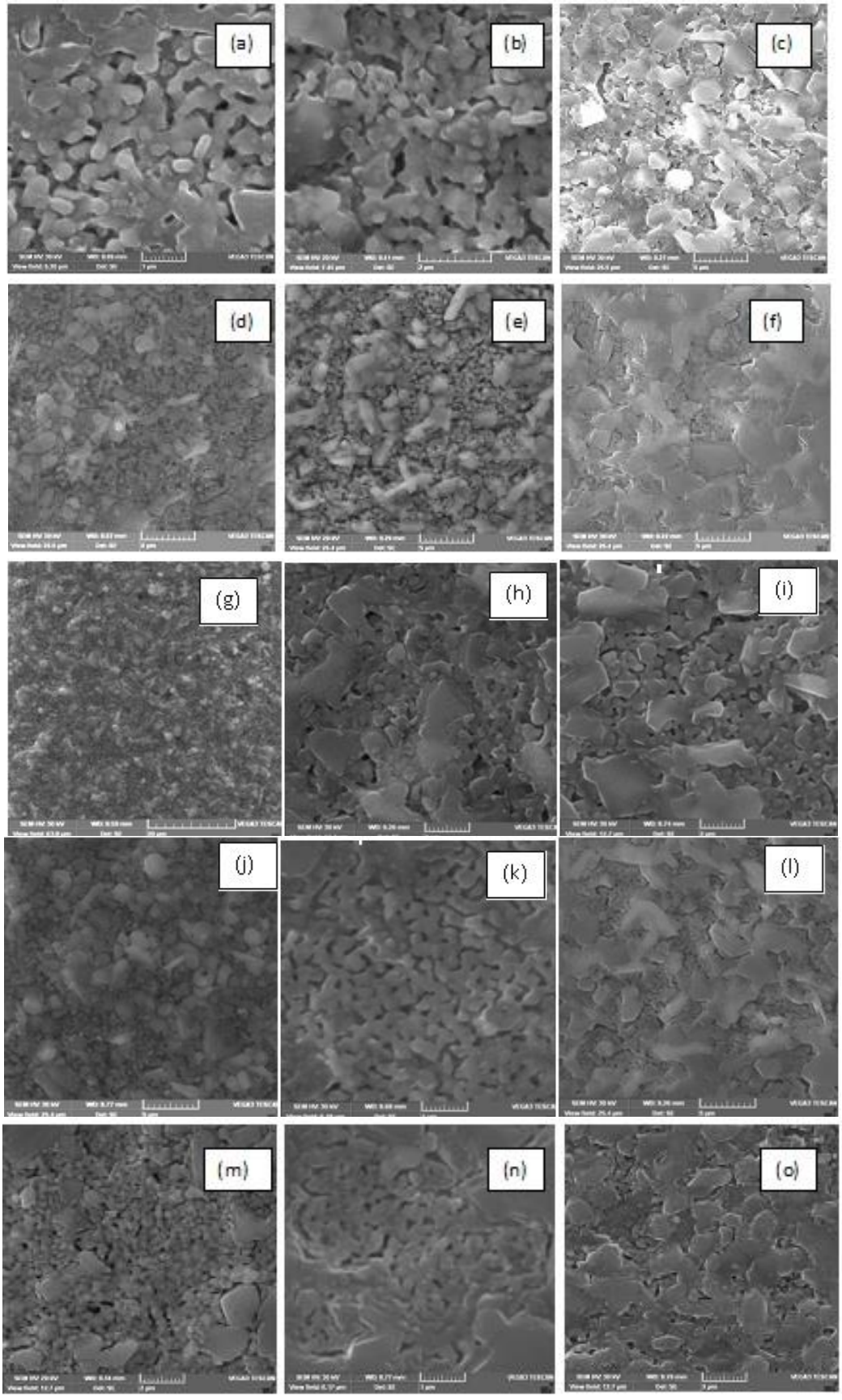

Fig. 7. SEM micrographs of conventionally sintered Al_2O_3 ceramics at different temperatures Batch I alumina (a)1450 °C (b)1500 °C (c) 1550 °C ; Batch II alumina (d)1450 °C (e)1500 °C (f) 1550 °C Batch III alumina (g)1450 °C (h)1500 °C (i) 1550 °C; Batch IV alumina (j)1450 °C(k)1500 °C (l) 1550 °C Batch V alumina (m) 1450 °C (n) 1500 °C (o) 1550 °C.

3.5 Dielectric studies

The dielectric constant of the ultrafine grained α-Al_2O_3 ceramics with MgO-Pr_6O_2-Gd_3O_2 as a function of its sintering temperature administered for a duration of 2 h. The variation of dielectric constant was dependable with that of density, except that the trend reversed at 1400 °C and was lower due to the nature of porosity. This was attributed to the incorporation of secondary phases in pure α-Al_2O_3 ceramics and the formation of magnesium, praseodymium and gadolinium oxide in to alumina.

For additive addition, MgO interacts with alumina during sintering where 3 Mg 2^+ ions with larger ionic radii replace 2 Al 3^+ ions of smaller ionic radii. Similarly Praseodymium and Gadolinium oxide with larger ionic radii replaces 2 Al 3^+ ions of smaller ionic radii [Table 3]. This causes increase in unit cell parameters and unusual expansion of unit cell volume of alumina.

Table 3. Physical property of experimental materials.

	Density g/cm^3	Ionic radius	Atom radius
Alumina	3.95	68 ppm	125 ppm
Magnesium oxide	3.58	85p pm	160p pm
Praseodymium oxide	6.9	85p pm	182 ppm
Gadolinium oxide	7.407	93.5 ppm	180 ppm

The ε_r increased with increasing sintering temperature and saturated at 4.9 to 8.7 for all the batches of various molar addition of magnesium, praseodymium and gadolinium oxide at the frequency of 1 MHz and it was observed in Fig. 8. The relationships between ε_r values and sintering temperatures reveal the same trend with those between densities and sintering temperatures since higher density was mainly a result from lower porosity[13]. The ε_r values rapidly increased from 4.9 at 1400 °C to 8.7 at 1550 °C for the well-sintered additive added alumina ceramics. In the case of pure and Boehmite added alumina ε_r values swiftly increased from 7.9 at 1400 °C to 9.8 at 1550 °C.

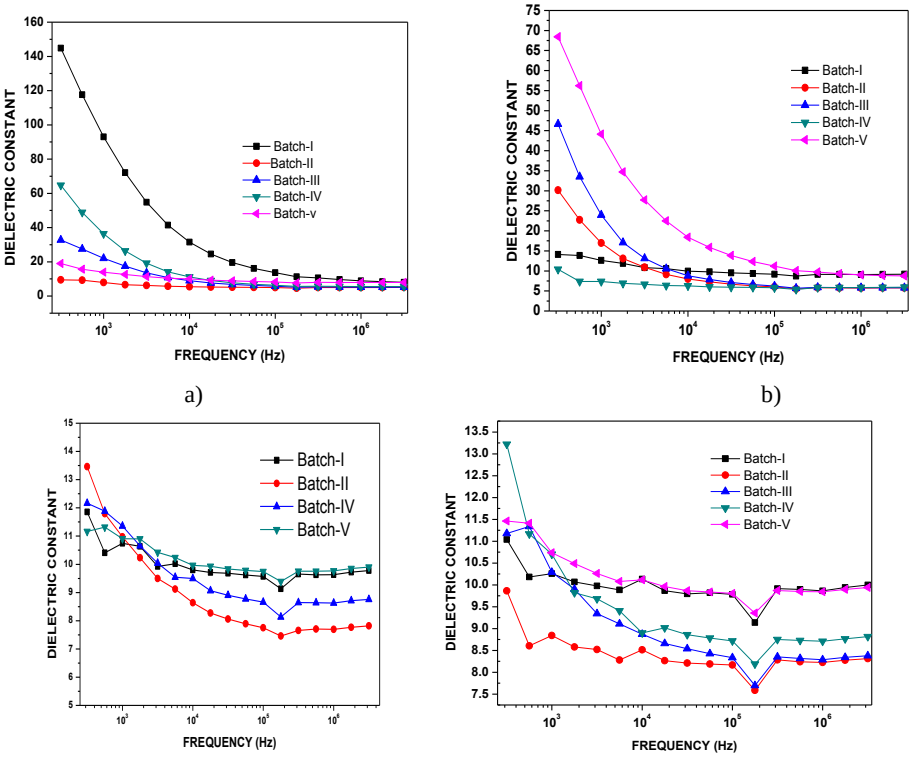

Fig. 8. Variation of dielectric constant as a function of frequency samples sintered at (a) 1400 °C (b)1450 °C (c) 1500 °C (d) 1550 °C.

Grain boundary segregation of dopants and impurities affects the microstructure development in substantial way. The addition of MgO enhances both the grain growth and densification rates during sintering of alumina ceramics, but at the same time efficiently suppresses abnormal grain growth (AGG).

Some Mg^{2+} ions are dissolved in the alumina crystal lattice forming point defect, but due to low solubility limits the concentration of dipoles is low. Rare earth elements are known as one of the additives that trigger AGG, and some works suggest that praseodymium forms vitreous phase at grain boundaries and the reaction with alumina matrix secondary crystalline phases, delay densification by grain boundary pinning.

The microstructure effects then prevail over the negative influence of point defects introduced into the alumina crystal lattice by dissolution of Pr and Gd^{2+} ions. Further increase of MgO codoped Pr_6O_2-Gd_3O_2 addition to 0.5 mol % significantly increased the loss tangent, which especially in the low frequency range was well above the values measured for pure alumina. This effect is attributed to the formation of spinel as a second crystalline phase in the material. Spinel particles segregate at grain boundaries, prevent densification, and increase the residual porosity of resulting material. This effect amplifies the influence of the diffusion of Mg with oxidation number 2^+ into the alumina crystals, creating lattice defects with resulting dipole effect. This hypothesis is further supported by the fact that the increase of loss tangent is reduced at high frequencies from 350 Hz to 3 MHz.

Similarly to Pr_6O_2 and Gd_3O_2 co doped MgO at the concentration of 0.5 mol % decreases the loss tangent under the level measured for pure. This observation is related namely to diffusion of Pr with oxidation number 2^+ and Gd with oxidation number 2^+ into the lattice, resulting in the formation of electric dipoles. The influence of the dipole effect on loss tangent is more pronounced at lower frequencies of external electric field shown in Fig. 9.

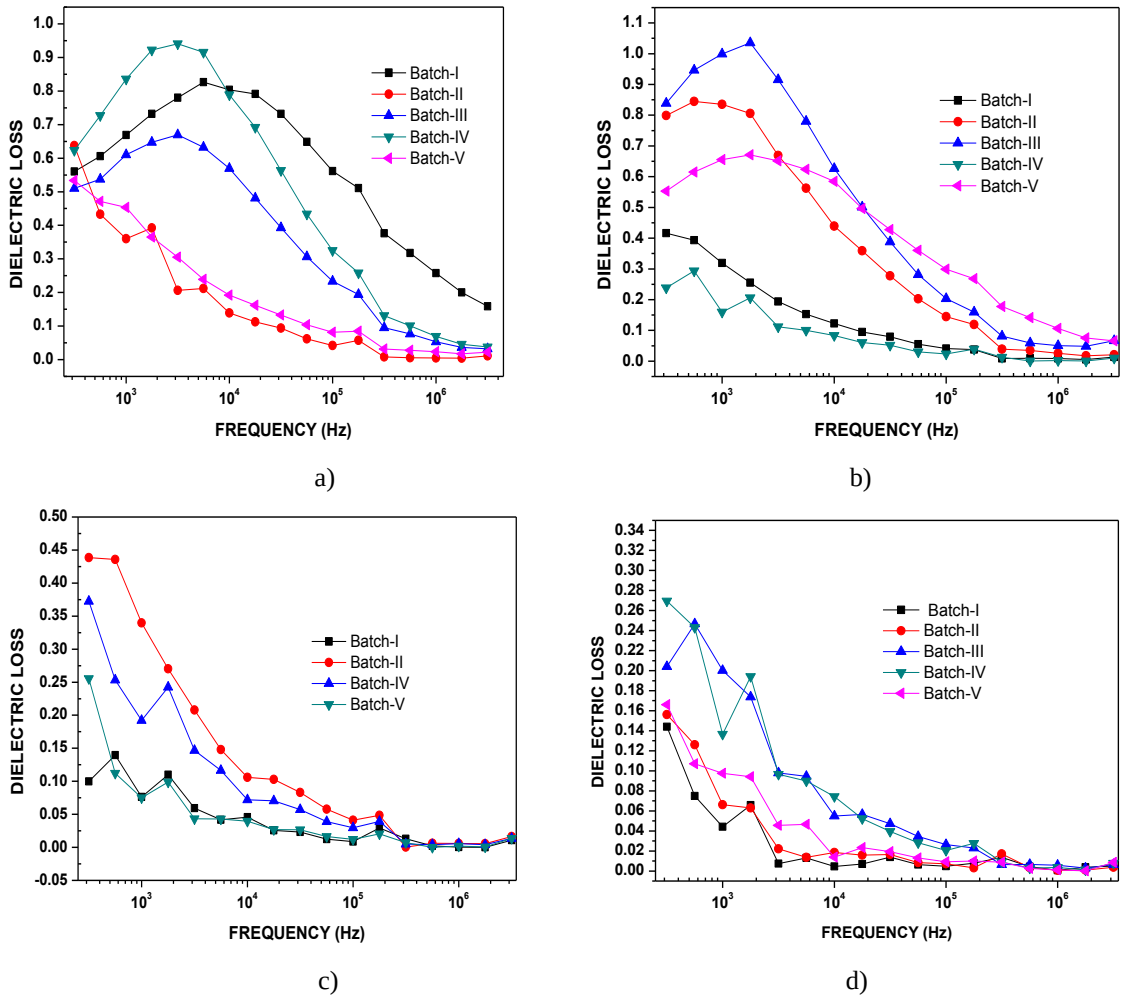

Fig. 9. Variation of Dielectric Loss as a function of frequency samples sintered at (a)1400 °C (b)1450 °C (c) 1500 °C (d) 1550 °C.

Since solubility of additives in the crystal lattice of Al_2O_3 is relatively small, the elimination of residual porosity and the presence of other phases play the main role in decreasing the loss tangent values. In the high frequency range the loss tangent is under the level measured for pure alumina. At 1400 °C the loss decreases from 2.5×10^{-1} (pure) to 5.1×10^{-3} in the case of MgO 0.5 mol % addition. It is observed that at 1450 °C the loss decrease from 8.8×10^{-3} to 1.84×10^{-3} by the domination of Gd addition in 0.5 mol %.Also at 1550 °C the loss decreases from 7.9×10^{-3} to 6.5×10^{-3} for the domination of MgO.

In the present investigation the measured value of a.c. resistivity for all the samples lies in the range 1.11×10^{12} to 2.27×10^{12} ohm cm. This higher value of resistivity is attributed to higher porosity. In fact, larger porosity which act as scattering centers for the flow of electrons and therefore increases the resistivity. It is also observed that the a.c. resistivity decreases with increasing temperature indicating the semiconducting nature of the samples. This is due to the increase in drift mobility of the charge carriers. According to Verwey's [14] hopping mechanism, the electrical conduction in alumina results from a hopping of the electrons between the ions of the same element, but of different valence states present at the octahedral site. It is known that magnesium, praseodymium and gadolinium ions occupy octahedral positions respectively. While alumina ion replaces by the extrinsic ions and develop crystal lattice defect and results in porosity hence the resistivity increases. In the case of pure alumina sintered sample at various temperature ranging from 1400 ºC to1550 ºC the obtained resistivity in the range of 1.14×10^{12} to 1.27×10^{12} ohm cm. But in the various amount of additive added (Batch I,II and III) sintered pellet at 1400 ºC due to the larger porosity the results of higher resistivity between 2.04×10^{12} ohm cm to 2.27×10^{12} ohm cm and at higher sintering temperature due to elimination of pores the resistivity decreases and it observed from Fig. 10.

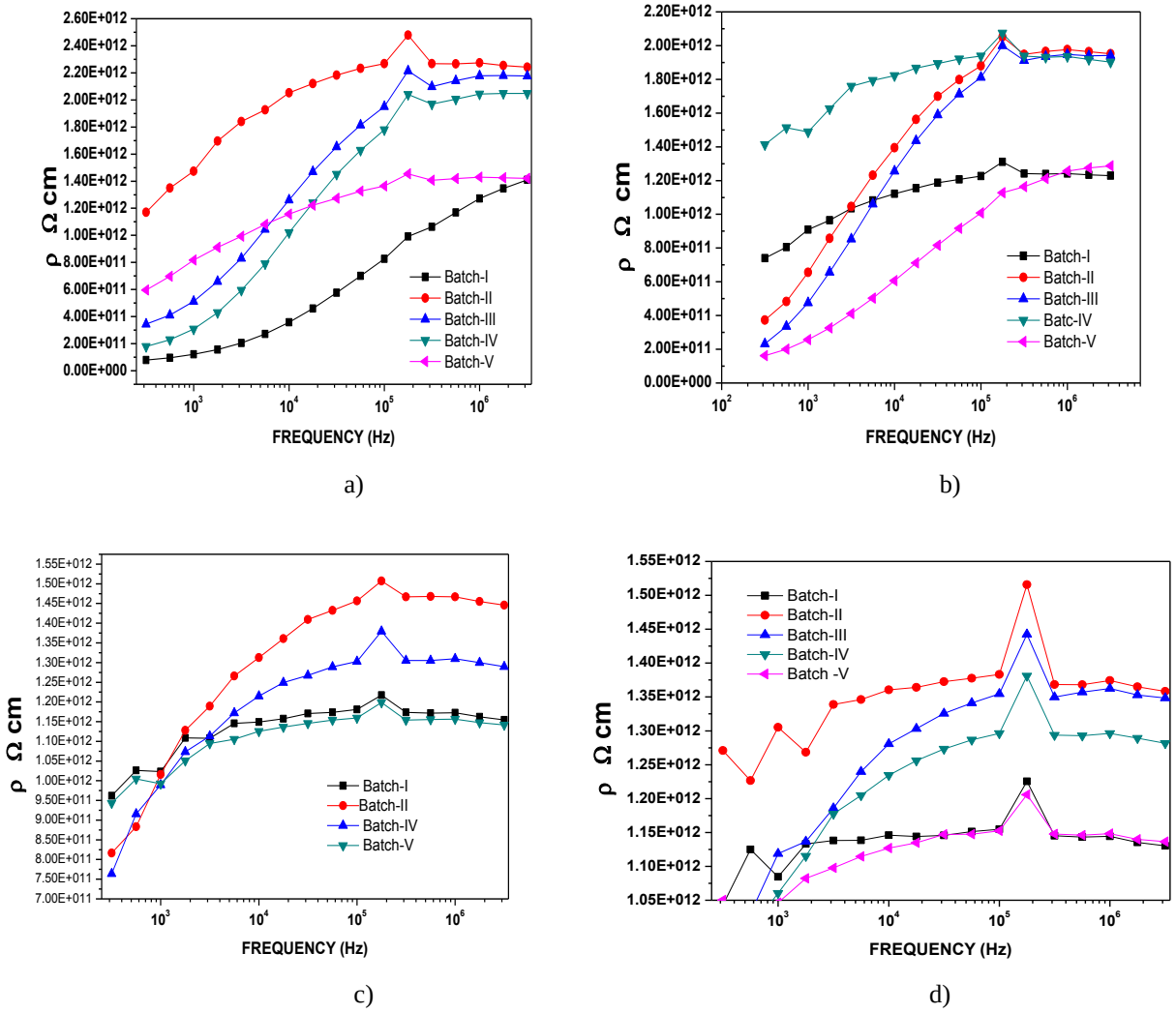

Fig. 10. Variation of resistivity as a function of frequency samples sintered at (a)1400 °C (b)1450 °C (c) 1500 °C (d) 1550 °C.

The variation of imaginary part of dielectric constant ε_r'' with log frequency at room temperature sample sintered at 1400 ºC to 1550 ºC is as shown in Fig. 11. At lower sintering temperature the materials achieved poor density and create more porous. In the porous region due to the greater polarization of the medium all electronic, ionic and orientation polarisation can orient themselves with the electric field at the lower frequency range, so as frequency of an applied voltage varied, the dipole response is limited and the dielectric constant make smaller. Further increase of temperature increase in grain growth, the porosity decrease and cause lower value of imaginary part of dielectric constant ε''.

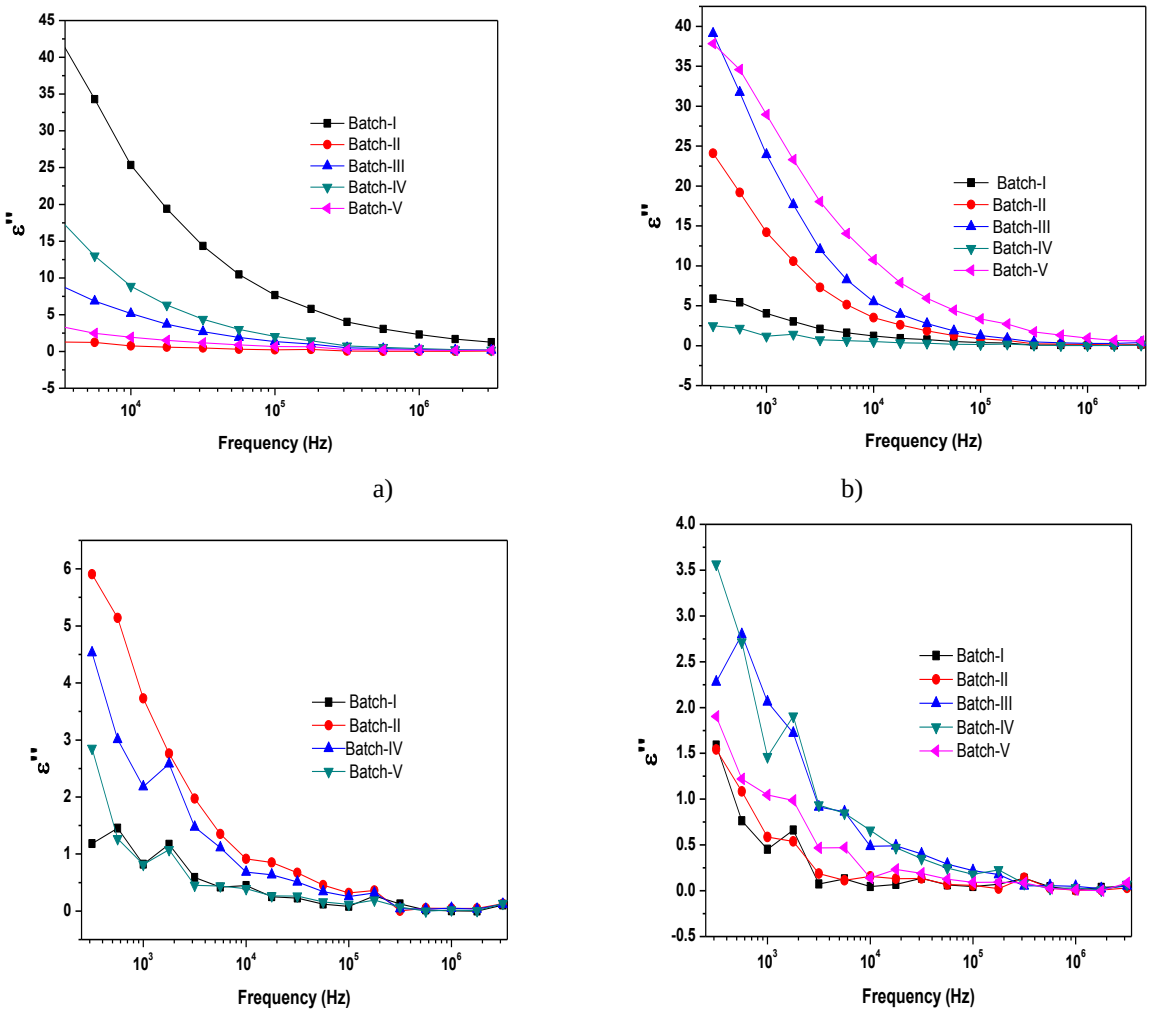

Fig. 11. Variation of imaginary part of dielectric constant ε'' with log frequency at room temperature samples sintered at (a)1400 °C (b)1450 °C (c) 1500 °C (d) 1550 °C.

4. Conclusions

The sintering behaviour and dielectric properties of ultra fine grained α-Al_2O_3 ceramics have been investigated in this paper. The dielectric properties are strongly related to relative density. In α-Al_2O_3, as the content of MgO, Pr_6O_2 and Gd_3O_2 in the green body increases from 0.3 mol % to 0.5 mol % in Al_2O_3 increases in volume shrinkage from 4 to 18% and decreases in porosity from 28 to 6%. For a pure α-Al_2O_3 sintered ceramics a low relative density of 81% was obtained at 1400 °C due to the porous specimen. However, the relative density increased and started to saturate at 1550 °C (relative density = 92%) with increasing sintering temperature. In the case of Batch I sintered material have a low relative density of 65% at 1400 °C and increase to 91% for the temperature of 1550°C. For Batch II at 1400 °C the relative density was obtained 64 % and increased to 92 % for the temperature of 1550 °C. From Batch III sintered sample observed that at 1400 °C the relative density was 67% and increased to89% for 1550 °C. For the Boehmite addition sintered pellet, the relative density improved from 87% at 1400 °C

to 98% at 1550 °C. The ε_r increased with increasing sintering temperature and saturated at 4.9 to 8.7 for all the batches of various molar addition of magnesium, praseodymium and gadolinium oxide at the frequency of 1 MHz.

At 1400 °C the dielectric loss decreases from 2.5×10^{-1} (pure) to 5.1×10^{-3} in the case of MgO 0.5 M% addition. It is observed that at 1450°C the loss decrease from 8.8×10^{-3} to 1.84×10^{-3} by the domination of Gd addition in 0.5M%.Also at 1550°C the loss decreases from 7.9×10^{-3} to 6.5×10^{-3} due to the domination of MgO.

The various amount of additive added (Batch II,III and IV) sintered pellet at 1400 ºC due to the larger porosity the results of higher resistivity between 2.04×10^{12} ohm cm to 2.27×10^{12} ohm cm and at higher sintering temperature due to elimination of pores the resistivity decreases.

References

[1] S. Bindra Narang et al., Journal of Ceramic Processing Research. **11**(3), 316 (2010).

[2] J. Ma et al., Thin Solid Films **462–463**, 477 (2004).

[3] S. Bindra Narang, Journal of Ceramic Processing Research. **11**(3), 316 (2010).

[4] C. K. Thomas et. al. Journal of Materials Processing Technology, **148**, 165 (2004).

[5] J. S. Throup et al., Journal of Materials science, **25**, 4143 (1990).

[6] Naoki Muraki et al., Polymer **43**, 1277 (2002).

[7] L. K. Namitha et al., Ceramics International **39**, 7077 (2013).

[8] Jin-min Chen, Ceramics International, **37**, 989 (2011).

[9] Jozef Chovanec, Ceramics International **38**, 2043 (2012).

[10] Soumen pal et al., Bull. mater. Sci., **33**(1), 55 (2010).

[11] Yung-Fu Hsu, Ceramics International **34**, 1183 (2008).

[12] A. V. Galakhov, refractories and industrial ceramics, **50**(5), (2009).

[13] Xiangming Li, International Journal of Refractory Metals and Hard Materials, Accepted date: 26 May 2013.

[14] J. W. Verwey, J. H. de Boer, Rec. Trav. Chim. Phys-Bas. **55**, 531 (1936).

*Corresponding author: rameshsrirangam@rediffmail.com